Universität Potsdam
Mathematisch-Naturwissenschaftliche Fakultät
Institut für Erd- und Umweltwissenschaften
Studiengang: Geoökologie

**Bachelorarbeit**

Organic matter composition of polygon-patterned tundra
in the Thule area (NW Greenland)

| | |
|---|---|
| vorgelegt von: | Torben Windirsch |
| Matrikelnr.: | 770855 |
| Telefon: | +49 176  61981242 |

| | |
|---|---|
| Gutachter: | Dr. Sebastian Wetterich |
| Zweitgutachten: | Dr. Frauke Barthold |

| | |
|---|---|
| Abgabetermin: | 10.11.2016 |
| Bearbeitungszeit: | 6 Monate |

**Table of contents**

## Table of figures

## Abstract

This thesis on organic matter composition of polygon-patterned tundra in the Thule are in Northwestern Greenland is based on analysis of a permafrost core obtained during an expedition of the Danish NOW project in August 2015. In the ice-sheet marginal coastal area in NW Greenland, Holocene ice-wedge polygons developed under permafrost conditions. The ice-wedge growth in accumulating peats linked to the presence of local sea bird colonies is the topic of this thesis. It was found that in the study area there is a high presence of nitrogen within the soil as well as very high ice content, linking to the syngenetic freezing and permafrost aggradation. The samples obtained from the core were processed in the laboratory and analyzed for ice content, age of the core, carbon and nitrogen content, threshold of organic carbon and isotopic abundance ratios of total organic carbon and total nitrogen. Analytical results show a quite steady content of all of these features with some exceptions at different depths for each parameter. It was also found that there had to be a change in permafrost aggradation and peat accumulation approx. 3000 years BP (before present, meaning before 1950) as the accumulation rate drops at this point in time. The great impact of the bird colonies on this specific permafrost formation is reflected as the high nitrogen values indicate that the birds' droppings were the original source of organic matter to decompose, allowing for vegetation growth and permafrost soil development. Temporary changes found in isotopic ratios within soil carbon may give a hint on bird colony evolution in the Thule area and the development towards the current state of the little auks' colony momentary inhabiting the study area of GL-3.

# 1. Introduction

## 1.1 Permafrost and periglacial landscapes

Permafrost, a term used for permanently frozen ground, is defined as any ground frozen solid for more than two consecutive years (Van Everdingen 2005). It is mainly made up of sediments, organic matter and ice and can be found in both Arctic and Antarctic non-glaciated regions around the globe as well as in alpine regions (**Figure 1**) (Brown et al. 2002; ESRI 2015). Different types of permafrost are distinguished by the percentage of ground being permanently frozen within a study area into continuous permafrost (> 90 % of the area is permanently frozen), discontinuous permafrost (50-90 %), sporadic permafrost (50-10 %) and isolated permafrost (< 10 %) (Brown et al. 2002). Permafrost is also distinguished into ice-rare and ice-rich permafrost, in which ice-rare means an ice content of less than 25 vol% whereas ice-rich refers to ice contents greater than 25 vol%.
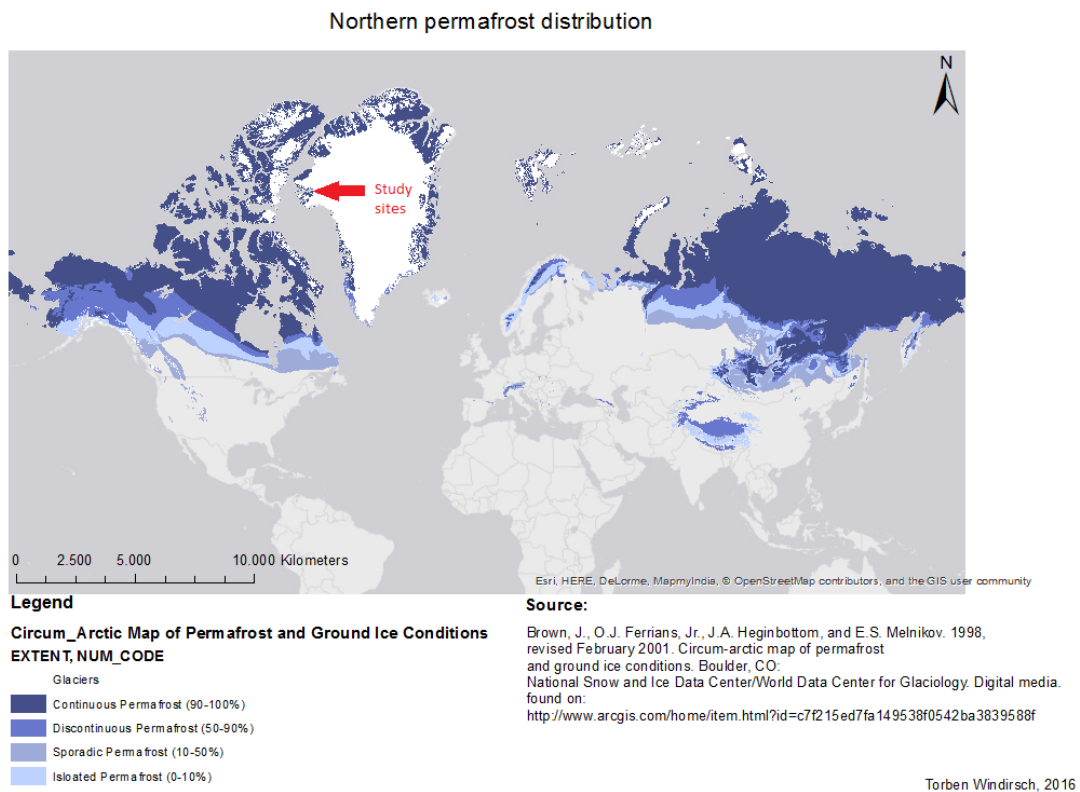


**Figure 1** – Permafrost distribution on the northern hemisphere. (Brown et al. 2002; ESRI 2015). The Thule area in NW Greenland is indicated by a red arrow.

There are specific permafrost patterns linked to permafrost-underlain ground, which form over time by consecutive thawing and freezing (cryogenic) processes and the resulting expansion and contraction of watery contents, i.e. ground water. These patterns make up the main appearance of periglacial landscapes. Patterned ground of periglacial landscapes develops over time spans of several hundred or thousand years, depending on the pattern looked at and the environmental requirements. There are various patterns known, such as circles, nets, steps, stripes, pingos, palsas and polygons (CRREL's Permafrost Tunnel Research Facility 2012). Ice-wedge polygons were studied and are further discussed in this thesis.

## 1.2 Ice-wedge polygon development

Ice-wedge polygons can be distinguished into low centered and high centered polygons. In the formation process of low centered polygons, liquid water during snowmelt in spring penetrates through frost cracks, which formed during winter, into the ground as a result of thermic contraction (**Figure 2-1**). Seeping down and freezing, vertical ice veins are formed and remain in the perennially frozen ground below the seasonally thawed uppermost active layer. In a consecutive year after repeated frost cracking when melt water seeps again, new ice veins form and result over time in a wedge-shaped ground ice body (**Figure 2-2**) in aggrading deposits. This process is called syngenetic permafrost aggradation and results in permafrost and ice wedges of approx. same age (French 2013). Expansion during freezing not only compresses the surrounding ground sideways but also upwards, forming a ridge (edge) above the growing ice wedge that delineates at the ground surface the polygon shape of the underlying ice wedges as low-center polygons (**Figure 2-3**) (Burn 1990) . High centered polygons form by ice wedge melt due to surface disturbance or changes in local hydrology or high sedimentation in the polygon center. The polygon ridge collapses and forms a through which allows liquid water to gather on top of the ice wedge. In spring, the ice-wedge surface gets covered by liquid water (**Figure 2-4**), which accelerates the melting process due to the great thermoconductivity of water (**Figure 2-5**). At this stage high centered polygons, which are the more recent form of permafrost polygons, are formed from these degrading low centered polygons once the melting in summer overweighs the ice gathering in winter (**Figure 2-6**) (Burn 1990; Fortier and Allard 2004).
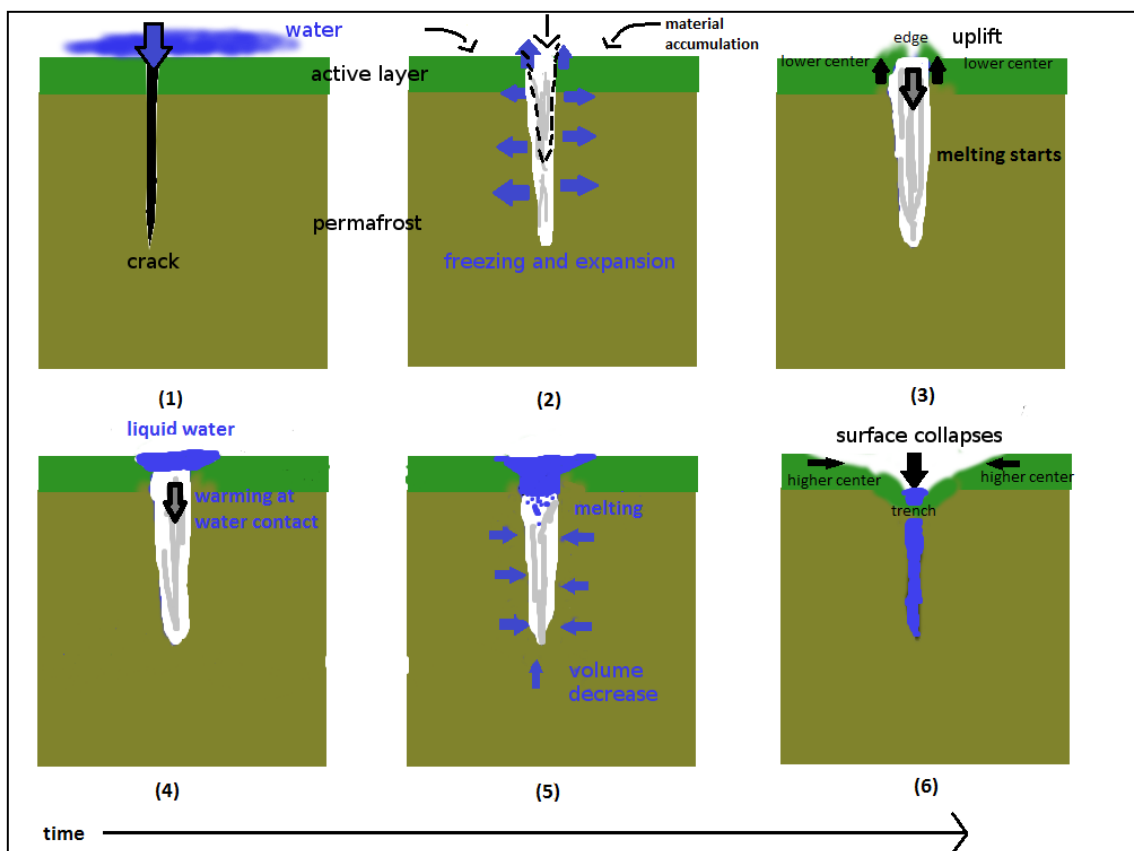


**Figure 2** – Schematic of ice-wedge and permafrost polygon development

## 1.3 Research aims

The thesis aims at **(1)** determining the evolution of ice-wedge polygons in the ice-sheet marginal coastal areas of North-Western Greenland, **(2)** characterizing the peat accumulation within these polygons and **(3)** showing the relation between the resident bird colonies providing nutrients for plant growth and peat accumulation in ice-wedge polygon tundra. To do so, various parameters of the permafrost composition were measured by laboratory analysis of permafrost samples obtained from drilling cores, in terms of ice content, radiocarbon dating, total carbon, total nitrogen, and total organic carbon threshold and isotopic abundance ratios of carbon stable isotopes and nitrogen stable isotopes.

## 2. Study area

All samples used in this thesis were taken in the Thule area in North-Western Greenland (**Figure 1 and 3**) in summer 2015 in the frame of the Danish The North Water (NOW) project (Cermak 2014).



**Figure 3** – Sample sites in the Thule area during the Danish NOW expedition in summer 2015 (Brown et al. 2002; ESRI 2015). The Great lake area (GL-3) core was obtained at the southernmost location of this expedition. Other sample sites are coded as Booth Sound (BS), Three Sister Bees (TSB), Saunders Island (SI) and Søkongedalen (SD).

## 2.1 Relief features

The area is shaped by mountainous surroundings and the former total glaciation of Greenland that lasted fully until approx. 11.000 years BP. Since then, deglaciation and the corresponding isostatic uplift of Greenland created a bedrock-dominated landscape of fjords. These deep fjords, carved into the landscape by once mighty glaciers lying directly on the shore, and the treeless coast allow a high influence of the surrounding Atlantic sea onto this area. Debris beaches and steep cliffs are the prevalent sight (Pohl and Zepp 1966). In Anguikitsoq, high centered polygons (up to 12 x 12 m) and trenches (up to 2m depth) are found to cover partly steep slopes, the lake catchment and the floodplain of the draining river. The exact sample site where the core examined in this thesis was obtained, in Anguikitsoq in North-Western Greenland in a place in the following referred to as Great Lake (GL-3), can be seen in figure 3. Cores were obtained at six sample sites in total during this expedition. A bird colony of little auks was found within short distance of the GL-3 sample site.

## 2.2 Climate conditions

Although Greenland is mainly characterized by a polar and subpolar climate, the west coast climate gets mellowed by the Western offshoot of the East Greenland Current, allowing for tundra vegetation to grow (DMI 2016). Wind directions are shifting fluently as the inland ice sheet prevents stabile wind conditions to develop (Pohl and Zepp 1966). It is a fully humid climate in which precipitation is mainly frozen throughout the year. Short summers with temperatures above 0 °C occur between June and August (**Figure 4**) (Climate-Data.org 2013), leaving a short vegetation period for plants to grow.
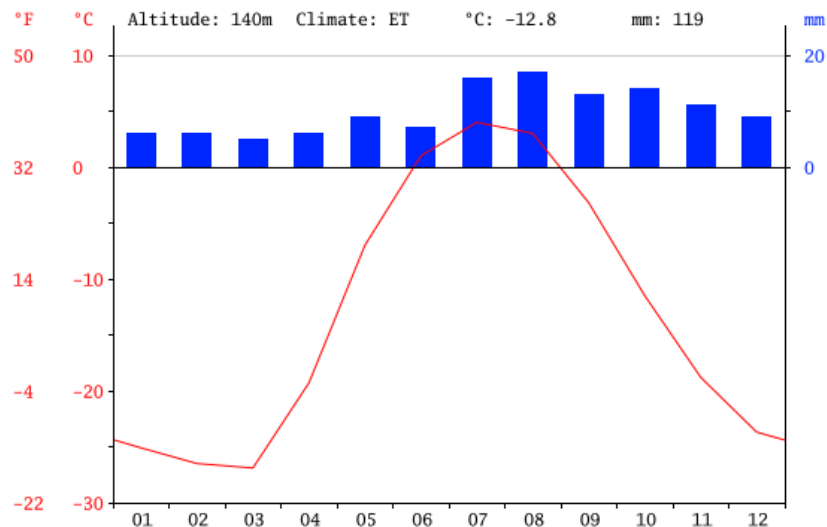


**Figure 4** – Climate of Thule, Greenland, 1982-2012 (Climate-Data.org 2013)

## 2.3 Permafrost conditions

Mapping data state that the area surrounding GL-3 is made up of continuous permafrost (Brown et al. 2002). An active layer depth between 20 and 25 cm was found in this area in August 2015. Also an ice wedge was found exposed in a trench next to the high centered polygon of GL-3, 1.2 m below the GL-3 surface, which was found to be fossil due to a melt surface, and the lack of recent frost cracks and ice veins. This ice wedge is made up of two different kinds of ice; ice-wedge ice containing numerous air bubbles < 1 mm in diameter, resulting in a whitish appearance, while the other is clear ice, assumed to origin from ponding water inside the trench (**Figure 5**). The smooth and rounded surface of the ice indicated a melting process from the top.
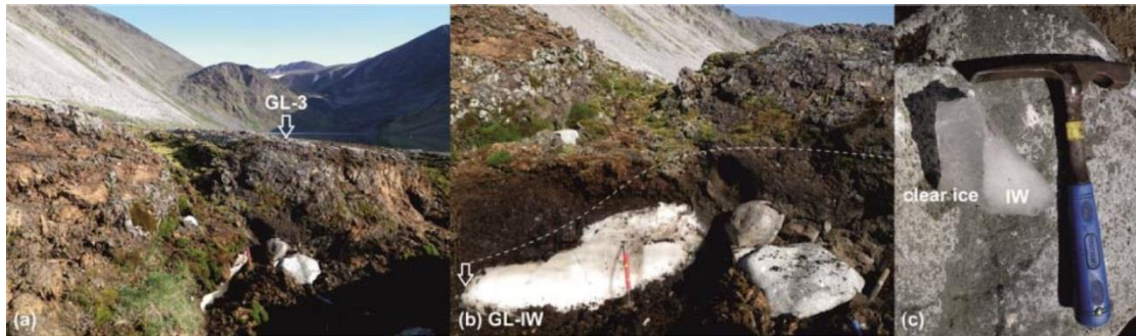
**Figure 5** – Ice wedge at GL-3, (a) sampling location, (b) close-up of position, (c) close-up of contact between whitish and clear ice (Photographs by S. Wetterich)

## 2.4 Vegetation

The vegetation of the GL-3 sample site is part of the Prostrate/ Hemiprostrate dwarf-shrub tundra (CAVM Team 2003), which is mainly made up of dwarf-shrubs (*Cassiope tetragona*). However, there were no shrubs found in this exact location, instead the local vegetation mainly consists of mosses, lichen, Cyperaceae (*Carex* sp.), Poaceae (*Alopercurus alpinus*) and Arctic mouse-ear (*Cerastium arcticum*). No trees and nearly no flowering plants are found surrounding GL-3.

## 3. Methods

In order to determine the characteristics of organic matter as well as cryogenic features the following paramteres were analyzed; ice content, contents of total carbon (TC), total nitrogen (TN), total organic carbon (TOC). Furthermore, the isotopic abundance ratios of total organic carbon ($\delta^{13}$C of TOC) were determined while samples for $\delta^{15}$N of TN analysis are still processed and therefore not presented here. Radiocarbon dating was applied to deduce accumulation ages of the studied peat sequence. The samples were processed using various measurement methods as given in the following (**Figure 6**).

## 3.1 Field work

The sample cores were obtained using a Snow, Ice and Permafrost Research Establishment (SIPRE) coring auger equipped with a STIHL BT-121 two-stroke engine (Zubrzycki 2012). This technique was used for the frozen ground parts while the samples from the unfrozen upper-most parts were dug by spade. The GL-3 core was obtained in the middle of a high centred polygon (**Figure 5a**) drilled to 320 cm below surface (BS). An active layer of 20 cm depth was found, composed mainly of the surrounding vegetation. The thawed peat of the active layer was found light-brown to brown, increasing over depth. The frozen section varied between brown and light-brown reddish. Cryostructures are mainly coarse lens-like (> 1 mm thick) while the peat is partly stratified (**Figure 7**).

## 3.2 Laboratory work

### 3.2.1 Sample preparation

The still-frozen cores were sawn at the climate chamber of GFZ Potsdam at approx. -8 °C with use of a Markita bandsaw. Drilled core pieces of 2 to 10 centimeters length were split lengthways giving two halves of each core piece. Those were cut every 2 to 4 cm into subsamples of which one of each subsamples was then sent to Aarhus University in Denmark for further survey and analysis such as radiocarbon dating while the others remained at AWI Potsdam.

### 3.2.2 Ice content determination

To determine the ice content of each subsample, the sample was weighed first, including the weight of the plastic bag it was packed in. Subsequently they were lyophilized using a **Zirbus Subliminator 3-4-5** freeze dryer and weighed again, still including the plastic bags. The weight-based ice content in wt% was then determinated by substracting the dry weight from the wet weight and then divided by wet weight, giving the wet-based ice content (**Equation 1**), and dry weight, giving the dry-based (**Equation 2**).

(1) *Wet-based ice content* $= \frac{wet\ weight\ (g) - dry\ weight\ (g)}{wet\ weight\ (g)}$

(2) *Dry-based ice content* $= \frac{wet\ weight\ (g) - dry\ weight\ (g)}{dry\ weight\ (g)}$

The ice contents are shown in **table 1**.

Due to very high ice contents in some layers and therefore resulting small sample masses, some of the samples had to be unified by mixing of adjacent samples in order to maintain a usable sample mass for further analysis. These layers are marked **brown** in **table 1**.

### 3.2.3 Sample division

For further studies and measuring the samples were first split again into two subsamples using a pincette and a spatula. In total, 75 samples were prepared for further analysis of the GL-3 core. The samples then were powdered using a **Fritsch pulverisette 5** -mill equipped with agate jars, each filled with the sample, three agate balls and then grinded twice for six minutes each run with 360 rotations per minute (rpm). The samples then were removed from the jars and transferred into 12.5 ml plastic jars for further storage using spatulas and a soft brush.

### 3.2.4 Radiocarbon dating

A spread selection of eleven samples was dated at the Aarhus AMS Centre at the Institute for Physics and Astronomy in Aarhus, Denmark (Aarhus AMS Centre 2015), using radiocarbon dating (C14) method. The results are shown in **figure 10**.

### 3.2.5 Total carbon and total nitrogen determination

Quantifying the total content of both TC and TN of the samples, each sample was prepared twice for measuring with an **elementar vario EL III** (varioEL) elementary analysis device. 5 to 5.8 mg, weighted on a **Sartorius micro M3P** scale (accuracy approx. 0.001 mg as stated by manufacturer) (Sartorius AG 2016), of each sample were put into tin capsules, combined with a small amount of tungsten(VI) oxide to catalyze the full combustion of the sample in the varioEL. To calibrate the measurement, a set of calibration standards consisting of acetanilide, sucrose and 30 % EDTA was used. Also every 15 samples, a control sequence of 30 % EDTA, 20 % EDTA, 12 % calcium carbonate, IVA33802150 (soil standard, C=6.7 %, N=0.5 %, S=1.0 %) and soil standard 1 (C=3.5 %, N=0.216 %) were measured.The measurement starts inside a combustion tube, provided with an oxygen-saturated helium atmosphere, at 1150 °C. Carbon dioxide, elemental nitrogen, nitrogen oxide and nitrogen dioxide are formed. In the following the nitrogen oxides are reduced inside a reduction tube filled with elemental copper at 850 °C, forming elemental nitrogen. Through gas chromatography the gases are split into their pure fractions, diluted in the helium atmosphere. At 50 °C the nitrogen fraction enters the measuring chamber, getting detected by a heat conductivity sensor. When all nitrogen has passed through and the amount, given as percentage from the initial weight-in, has been measured, the chamber gets heated up to 130 °C and the former formed carbon dioxide enters the measuring

chamber, getting measured in the same way (Kempf 2005) to determine the TC content. The TC and TN values are given as wt%. The accuracy of the measurement was ± 0.1 % for nitrogen and ± 0.05 % for carbon.

### 3.2.6 Total organic carbon determination

To differentiate the total organic carbon (TOC) content, the samples are measured using an **elementar varioMAX C** elementary analysis device. This device works on catalytic tube pyrolysis using nitrogen as carrier gas (purity of 99.996 %). In this measurement, the sample mass to use is calculated from the total carbon content, giving in this case values between 15 and 20 mg, weighted on a **Mettler Toledo XS105 dualrange** scale (accuracy of 0.1 mg as stated by manufacturer), which are filled into steel crucibles. 30 % glutamate, pure glutamate and 2:3 glutamate are used to calibrate the measurement. The control sequence consists of 2:3 glutamate, 10:40 glutamate, 5:45 glutamate and 1:19 glutamate, which is again placed between each 15 samples.

The samples get burned inside the crucibles at 580 °C under use of oxygen (purity of 99.995 %) to give pure carbon dioxide and are then further heated to 930 °C to enable complete combustion.Detection takes place in either one of the two detection tubes in which one is more sensible, used for carbon contents of up to 2 %, while the other is less sensitive and is used for carbon contents > 2 %. To determine the carbon dioxide peak during integration, the cut off value is calculated from parameters such as sample mass and expected carbon content. Value and occurrence time of this peak enable to determine the total amount of organic carbon (Information provided by manufacturer in manual). The accuracy of the measurement was ± 0.1 %. Subsequently a ratio is calculated from TOC and TN, referred to as C/N, to determine the decomposition state of the organic matter, in which high ratio values indicate a mainly undecomposed organic share.

### 3.2.7 Isotopic abundance ratios of carbon and nitrogen

In preparation for stable isotope analysis, carbonate ions must be removed from the samples. To do so, approx. 2 g of each sample, less if the total sample mass was below 2 g, were weighted using a **Sartorius MSU 224S − 000 − DU** scale (accuracy 0.1 mg as stated by manufacturer) (Sartorius AG 2016), and transferred into 100 ml Erlenmeyer glass flasks. They then were dosed with each 20 ml 1.3 molar hydrochloric acid and heated at 97.7 °C for 3 hours. During this process, the carbonate ions react following the given chemical equation (**Equation 3**, carbonate removal reaction ('Carbonat-Nachweis nach Kohlendioxidentwicklung' 2009)).

**(3)** $CO_3^{2-} + 2\,HCl \rightarrow CO_2 + 2\,Cl^- + H_2O$

Field work

Laboratory work

Sampling

Ice content determination

Sample division

Main sample

Radiocarbon dating (C14)

Milling

Total carbon and nitrogen determination (TC/TN)

Total organic carbon determination (TOC)

Removal of Carbonate ions

Isotopic abundance ratios

carbon stable isotopes (δ13C) of TOC

nitrogen stable isotopes (δ15N) of TN
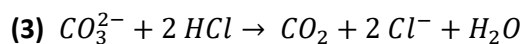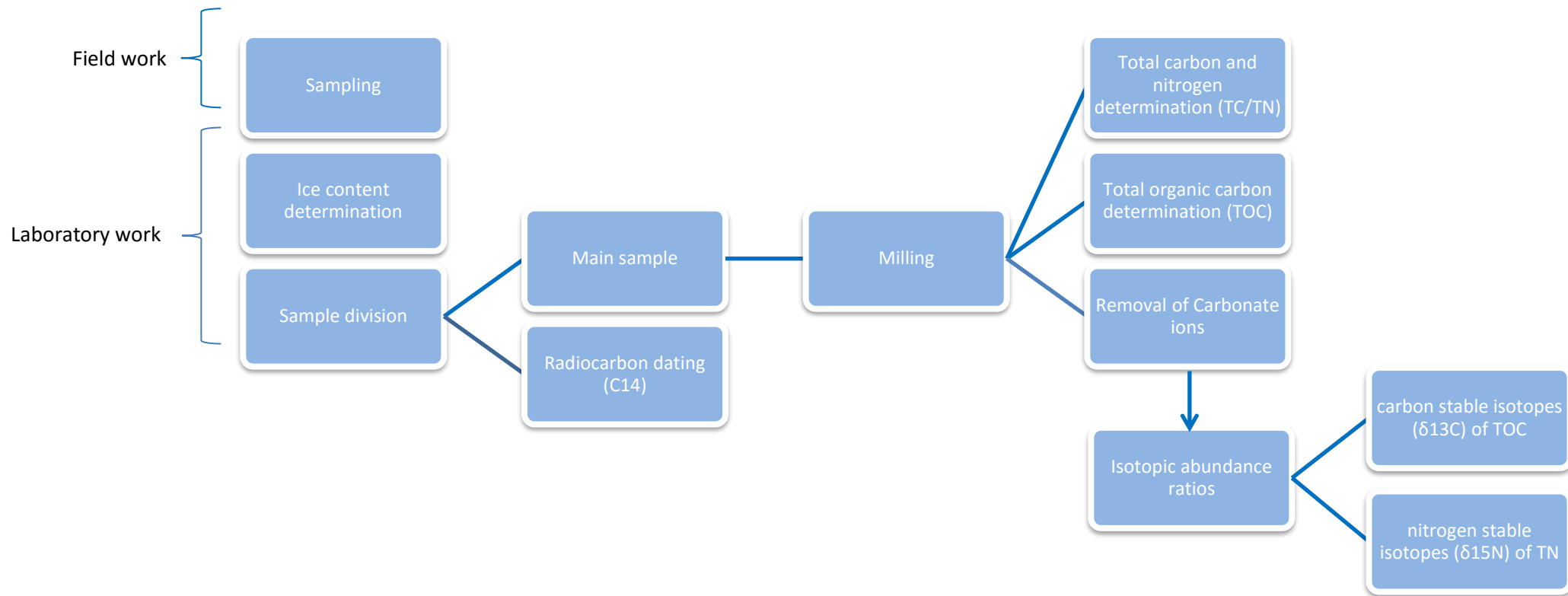
**Figure 6** – Overview scheme of analytical processes applied to the sample material of core GL-3
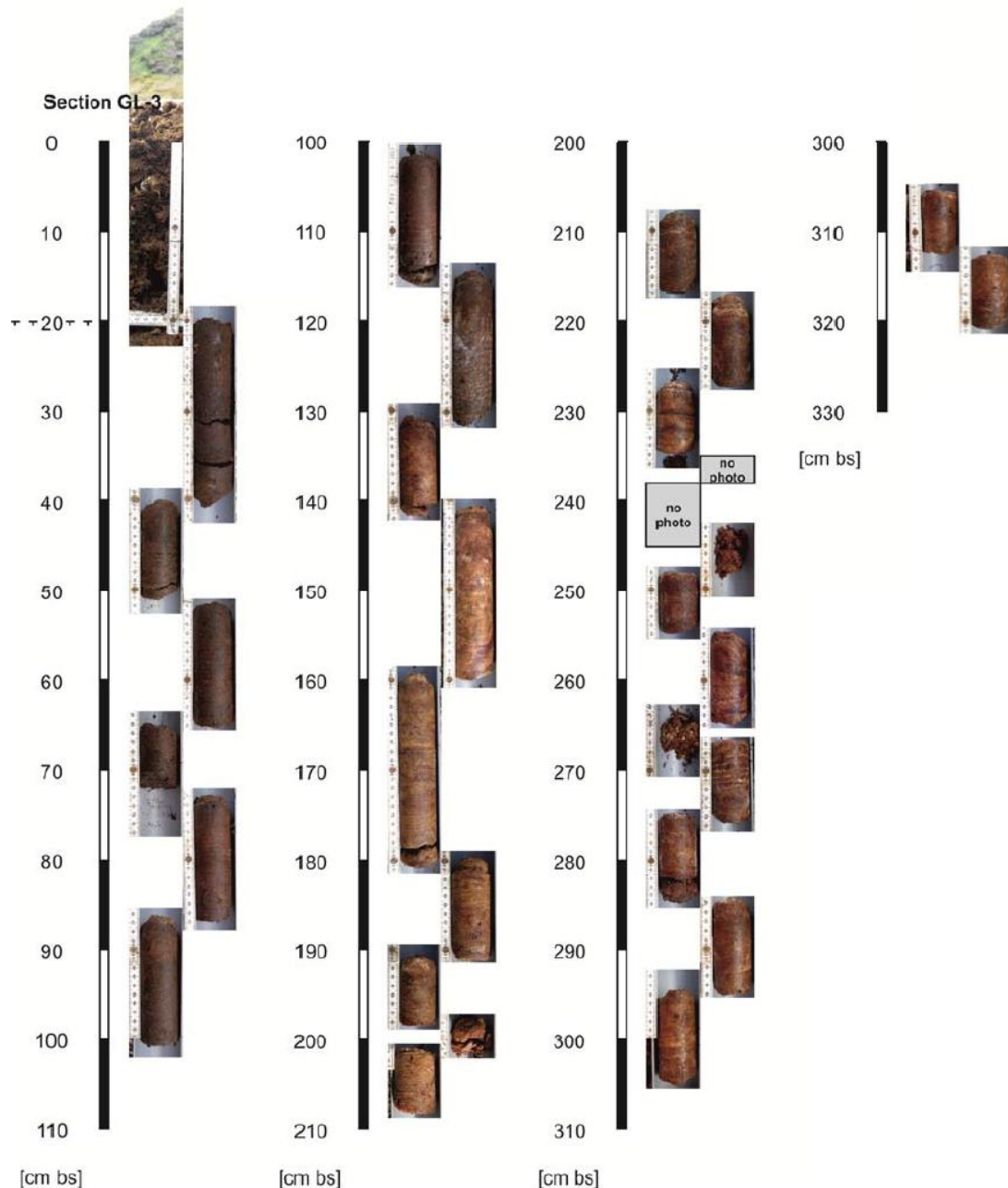
**Figure 7** – Field photographs of drilled sections of the GL-3 core showing its' appearance over depth (cm BS)

To get rid of the Cl⁻ ions originating from the hydrochloric acid, as they would trouble the isotope analysis, the flasks were filled up with purified water and let rest in order for the sample to sediment. This process was repeated until the sample contained less than 500 ppm Cl⁻. This was tested using **Quantofix Chloride** test strips (mbm-lehrmittel 2014). To regain a dry sample state, sample solution was then filtered under vacuum using **GE Healthcare Life Sciences Whatman glass microfiber filters** (GE Healthcare Life Sciences 2016). The sample then was dried at 50 °C and subsequently pestled by hand before being transferred into 12.5 ml plastic jars. Preparation for measurement was executed by placing the samples in tin capsules, where each target weight was calculated (**Equation 4** for $\delta^{13}$C, **Equation 5** for $\delta^{15}$N).

**(4)** $target\ weigh - in = \frac{20}{TOC}$

**(5)** $target\ weigh-in = \frac{10}{TN}$

The actual weigh-in was carried out with an accuracy of 0.1 mg referring to the target weigh-in using a **Sartorius micro M3P** scale (accuracy of 0.001 mg as stated by manufacturer). Analysis was realized using a **Thermo Scientific Delta V Advantage Isotope Ratio MS** supplemented with a **Flash 2000 Organic Elemental Analyzer** using helium as a carrier gas.

In this, the first analysis step is the sample combustion and oxidation at 1020 °C with $CrO_2$ as an oxidant, resulting in the formation of $CO_2$ and $NO_x$. These products then get reduced at 650 °C using elemental copper (Cu), leaving the $CO_2$ unchanged but forming elemental nitrogen ($N_2$) from the $NO_x$. To separate these gases, a gas chromatography tube is used to elongate the way the gases have to pass. Separation happens as the nitrogen molecules are lighter and therefore faster than the $CO_2$, allowing the nitrogen to enter the mass spectrometer unit earlier than the $CO_2$. Inside the mass spectrometer unit, elemental nitrogen from external source is measured as reference, followed by the nitrogen partition of the sample. Once the nitrogen has passed through, the carbon dioxide reaches the mass spectrometer unit, gets measured and is followed by external supplied $CO_2$ for reference. The actual method of measurement is to ionize the sample or reference gas by inducing energy by electron impulse. Then the analysis unit separates the ions by mass/charge ratio, followed by the intensity being detected at the detection unit (Wiley Information Services GmbH 2016).The measured values are linearly corrected using reference sample. The accuracy of this measurement was better than ± 0.15 ‰ for carbon and was not fully carried out for nitrogen due to technical issues.


## 4. Results

### 4.1 Organic matter characteristics of the GL-3 permafrost core

The measured values for ice content, radiocarbon dating, TC, TN, TOC, C/N and $\delta^{13}C$ of TOC (**table 1**) were plotted over drill depth using the **Grapher Golden Software package 7** (Golden Software, LLC 2016). The overall ice content varies between 61.7 wt% and 86.6 wt% (wet-based). However, there is a decrease in ice content on the surface of the core (39.1 wt% wet-based) as well as a negative peak at 265-267 cm BS (**Figure 8-1**) with a content value of 56.8 wt% ice (wet-based).

TC varies between 42.7 wt% to 48.4 wt%, in which the upper part varies between 45.7 wt% and 48.4 wt%, while the lower part includes values between 42.7 wt% and 46.8 wt%. It shows a steady trend with a slope change at 140 cm BS and a positive step at 224-227 cm BS (46.1 wt% to 46.8 wt% to 45.5 wt) (**Figure 8-2**). The upper part down to approx. 140 cm BS varies around 47 wt% while the lower part is around 45 wt%.

The TN values range from 0.5 wt% to 1.9 wt%. They show a slight decrease from the surface to the bottom of the active layer at 20 cm BS from 1.8 wt% to 0.9 wt%, an increase at 224-227 cm BS from 1.5 wt% to 1.9 wt% and a slight increase at the core bottom from 309 to 320 cm BS (1.2 wt% to 1.6 wt%) (**Figure 8-3**).

TOC values correspond to the TC values and range from 42.1 wt% to 48.8 wt%. They contain a slightly variable part between 70 and 140 cm BS (**Figure 8-3**) compared to the TC values. The upper part down to approx. 140 cm BS varies around 47 wt%, the lower varies around 44 wt%.

C/N varies between 24.7 and 91.7 and reaches its peak at 127-131 cm BS with a value of 91.7 and decreases in both directions from this point (**Figure 8-4**). The slope change of TOC is also visible but the C/N values cannot be clearly divided into two different slope parts.

$\delta^{13}$C of TOC values vary between -26.59 ‰ and -20.73 ‰ and show unsteadiness from 60 to 160 cm BS, varying between -25.64 ‰ at 99-102 cm BS and -22.34 ‰ at 153-157 cm BS (**Figure 8-5**). The negative maximum can be found at 224-227 cm BS with a value of -26.59 ‰. A negative trend can be seen at the end of the core, starting at approx. 285 cm BS and reaching down to 320 cm BS, including the highest overall value of 20.73 ‰ at 300-305 cm BS.

The ages of the different layers present a younger age for the top layers where the youngest dated layer is about 652 years BP, and an older age for the deeper layers of about 3855 years BP, with an age back step at 267-271 cm BS (**Figure 9**). There is a less steep part between 5-10 cm BS and 48-52 cm BS than in the rest of the core. (R Core Team 2016).
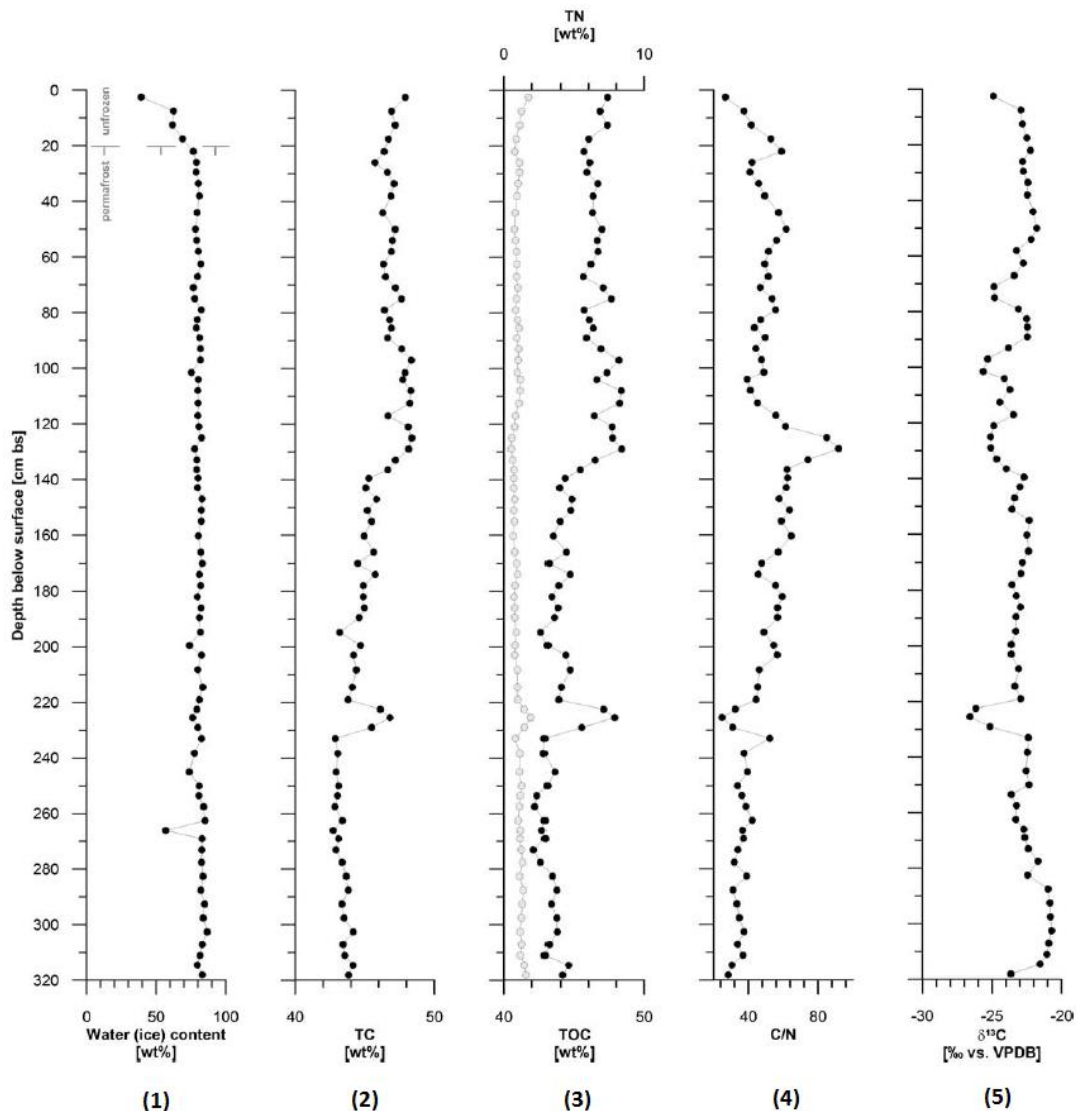


**Figure 8** – Measured values of ice content, TC, TN, TOC, C/N and $\delta^{13}$C over depth of the GL-3 permafrost core (Golden Software, LLC 2016)
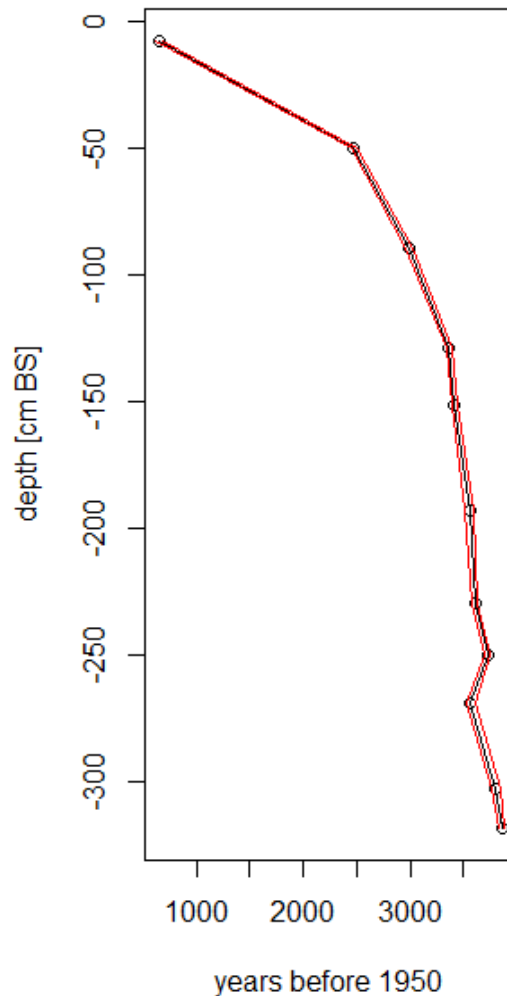
**Figure 9** – Uncalibrated radiocarbon dates of GL-3 over depth, given as years before 1950 standard deviation given in red (R Core Team 2016)


**4.2 Data interpretation and context integration**

The measured ice content of about 80 wt% wet-based indicates an increased water flow as it had to infiltrate into the ground to form ice. This water may result from snow melt or higher precipitation in summer (**Figure 4**). The partly high ice contents around 80 wt% may indicate warm summers, enabling water to maintain a liquid state and infiltrate into the ground. If otherwise summers had been around 0 °C we would expect lower ice contents within the core.  The decrease in ice content in the active layer origins from the fact that it is no real ice content but rather moisture content as the active layer is not permanently frozen but was thawed up in August 2015 when the samples were obtained.

Due to the slope change at 140 cm BS in TC, TOC, C/N and $\delta^{13}$C values (**Figure 8**), the core can be divided into two main parts, indicating a change in environmental influences approx. 3000 years BP (**Figure 9**).

When calculating the difference between TOC and TC there are negative values which indicate that there is no inorganic carbon present or in other words that all carbon present is organic carbon.

However, then the differences should be equal to zero, but the negative values may result from an unlucky appearance of measurement inaccuracies within the standard deviation.

TN values as well as the TOC/TN ratio may show that in the past the active layer was either shorter exposed on the surface and sooner overlain by new material or the temperatures throughout the summer were colder, preventing the organic matter to be decomposed, which could probably be related to global warming. The higher TN values in the active layer indicate that organic matter in this area has been less decomposed than in the areas below (**Figure 8-3**). This can be seen in the TOC/TN ratio in the surface area as well (**Figure 8-4**). If it had been more decomposed, the nitrogen would have degassed resulting in lower TN values within the active layer (Strauss et al. 2015; Gundelwein et al. 2007). The less steep part in the top section of figure 9 indicates a slower peat accumulation rate within the last 2900 to 3000 years than before. The back step at 267-271 cm BS means that there is older ground material overlaying younger material.

## 5. Discussion

### 5.1 Peat accumulation and ice-wedge growth over time

The oldest obtained radiocarbon age of 3855 ± 30 years BP from the lowermost core sample (drill depth of 316 to 320 cm BS) confirms at least subboreal to subatlantic permafrost and peat aggradation during the late Holocene. Since the drilling stopped at this depth because of rock presence in the underground (personal communication S. Wetterich), the age might further indicate the onset of peat formation in the study area. The rather well-established age-depth relation of GL-3 allows to assume a continuous sequence preserved in the core. The permafrost aggraded syngenetically within accumulating peat subsequently turned into permanently frozen state and preserved. The seasonally unfrozen uppermost active layer depth is assumed to experience only little variation over time. Peat accumulation was rapid between 320 and 130 cm BS for about 500 years (between 3855 ± 30 and 3365 ± 28 years BP), while the uppermost 130 to 0 cm BS accumulated within more than 3000 years (between 3365 ± 28 and 0 years BP) if no hiatus is assumed (**Figure 9**). The substantially lower accumulation rate of the uppermost 130 cm of the GL-3 permafrost core may be due to either less bird activity, resulting in fewer droppings, providing fertilizer and soil-building material, or in a change in plant activity, so that more carbon rich material is transformed into vegetation matter by a gain in plant growth.

The age inversion within the timeline at GL-3-267-271 cm (3568 ± 39 years BP) cannot be fully explained, but possibilities are that younger material has been pressed into the older layers by animal activity, e.g. musk oxen, or the collapse of an adjacent polygon edge relocating younger material into the polygon center, or by a temporary increase in cryoturbation. However, none of these possibilities can be proven.

The negative peak at 265-267 cm BS in ice content (**Figure 8-1**) can possibly be traced to a dry period with less precipitation which resulted in less obtainable water for ice formation. Other papers based on Greenlandic climate state not a dryer but colder climatic situation about that time, also resulting in less obtainable, liquid water (Fredskild 1983). As there are no exact climate data from this time period available, this would have to be proven by examining ice content in the surrounding areas in soils of similar age.

There is a remarkable step in carbon and organic carbon content at approx. 230 cm BS, as well as in C/N and $\delta^{13}$C ratios. This means that there had to be an external temporary organic carbon source which cannot be further determined. However, usually peaks in C/N and $\delta^{13}$C are opposed to each other, but are parallel in this case. Therefore the isotopic footprint of this organic matter does not exactly match the area's isotope ratio. All these indicators support the theory of an external organic matter source different from the usual sources.

## 5.2 Co-evolution of bird colonies and polygons over time

The high nitrogen shares within the permafrost samples and the overall presence of little auk colonies lead to the assumption that a high percentage of the ground's organic matter originates from bird droppings and resulting fertilization of moss vegetation as there is no other plausible source of nitrogen-rich organic matter around. The fact that when preparing the samples for analysis using hydrochloric acid fast and spontaneous degassing took place supports this hypothesis, as sea birds like the little auks mainly consume shellfishes which contain a high amount of calcium carbonate that leads to this reaction. As the surrounding areas are chiefly dominated by blank bedrock and the Greenlandic inland ice, the bird colonies are the natural choice for an organic matter source. That means, that, as far as we can assume, the largest share of the organic matter within the permafrost is related to the bird colonies and therefore polygon development started with the arrival of the first bird colonies within this area. Plants developed within the active layer of the arising permafrost making the area more habitable for birds as they provide i.e. nesting material.

The possible external carbon source found at 230 cm BS could give a hint on the evolution of bird colonies in the greater surrounding area. It is possible that a different sea bird species than the little auk nested in the area temporarily, leaving a different isotopic ratio as they probably feed farer off the coast or on different fish or shellfish. Wagner and Miller state in a paper on bird colony development in Greenland that due to a temporary cold event (Fredskild 1983) the climate was harsher so other, larger bird species that are not typical for Greenland nested on the cost rather than on small island in the open sea (Wagner and Melles 2001). This may lead to the different isotopic ratio as well as it describes the states the local bird colonies have gone through.

Also the decrease in accumulation rate could possibly link to a change in bird activity such as bird count and colony size. Perhaps the deglaciation and warming of the Greenland area allowed to inhabit smaller island in the open sea for little auks, resulting in decreasing colony sizes and fewer droppings and therefore slowing down the permafrost accumulation rate.

## 6. Outlook

The present study shows that there are some uncertainties regarding e.g. the bioactivity on top of and within the active layer and the change in peat accumulation 3000 years BP.

The Danish NOW project (Cermak 2014) is examining these changes in terms of human civilization and activity that may have led to named changes.

Furthermore, there were more cores obtained than used for this thesis. These permafrost areas within the Thule are built up under influence of different bird colonies and different species of birth. To validate the findings of this thesis regarding the influence of bird colonies on permafrost soils, these cores have to be analyzed as well.

The ice wedge found at GL-3 has also been examined but results have still to be put in context.

Participants of the NOW project are also working on the bird colonies' development and the reasons for and conditions of bird colonies within the Thule area.

Due to technical issues, the isotopic abundance ratios of TN were not available by the time this thesis was submitted. However, the samples will still be processes and the findings will be further analyzed.

## 7. References

Aarhus AMS Centre, Jan Heinemeier. 2015. 'Aarhus AMS Centre'. *The Centre - Institut For Fysik Og Astronomi*. http://phys.au.dk/forskning/forskningsomraader/aarhus-ams-centre/the-centre/.

Brown, J., O. Ferrians, J. A. Heginbottom, and E. Melnikov. 2002. '| National Snow and Ice Data Center'. *Data Set ID: GGD318 Circum-Arctic Map of Permafrost and Ground-Ice Conditions, Version 2*. https://nsidc.org/data/ggd318.

Burn, C. R. 1990. 'Implications for Palaeoenvironmental Reconstruction of Recent Ice-Wedge Development at Mayo, Yukon Territory'. *Permafrost and Periglacial Processes* 1 (1): 3–14. doi:10.1002/ppp.3430010103.

'Carbonat-Nachweis nach Kohlendioxidentwicklung'. 2009. *Praktikum Anorganische Chemie/ Carbonat*. https://de.wikibooks.org/wiki/Praktikum_Anorganische_Chemie/_Carbonat.

CAVM Team. 2003. 'Circumpolar Arctic Vegetation Map (1:7,500,000 Scale), Conservation of Arctic Flora and Fauna (CAFF) Map No. 1. U.S. Fish and Wildlife Service, Anchorage, Alaska. ISBN: 0-9767525-0-6, ISBN-13: 978-0-9767525-0-9'. *Circumpolar Arctic Vegetation Map*. http://www.arcticatlas.org/maps/themes/cp/.

Cermak, Astrid. 2014. 'The Now Project: Living Resources and Human Societies around the North Water in the Thule Area'. November 3. http://now.ku.dk/.

Climate-Data.org. 2013. 'Klima Thule'. *Climate Thule 1982-2012*. http://de.climate-data.org/location/219893/.

CRREL's Permafrost Tunnel Research Facility. 2012. 'CRREL's Permafrost Tunnel Web Site: Permafrost: Patterned Ground'. *Permafrost: Patterned Ground*. http://permafrosttunnel.crrel.usace.army.mil/permafrost/patterned_ground.html.

DMI. 2016. 'Klimanormaler for Grønland'. *Klimanormaler for Grønland*. http://www.dmi.dk/groenland/arkiver/klimanormaler/.

ESRI. 2015. *ArcGIS Desktop: Release 10.3.1* (version 10.3.1). Redlands, CA: Environmental Systems Research Institute.

Fortier, Daniel, and Michel Allard. 2004. 'Late Holocene Syngenetic Ice-Wedge Polygons Development, Bylot Island, Canadian Arctic Archipelago'. *Canadian Journal of Earth Sciences* 41 (8): 997–1012. doi:10.1139/e04-031.

Fredskild, Bent. 1983. *The Holocene Vegetational Developement of the Godthabsfjord Area West Greenland*. Museum Tusculanum Press. https://books.google.de/books?id=DzDxjthx7rgC&printsec=frontcover&hl=de&source=gbs_ge_summary_r&cad=0#v=onepage&q&f=false.

French, Hugh M. 2013. *The Periglacial Environment*. John Wiley & Sons. https://books.google.de/books?hl=de&lr=&id=GPuhmEgR-MoC&oi=fnd&pg=PT32&dq=The+Periglacial+Environment+French+third+edition&ots=tIi9iQcTgu&sig=3ScZ7tdodNPxn8_zxZHj21heZ4I.

GE Healthcare Life Sciences. 2016. 'Grade GF/B Filter for Liquid Scintillation'. Web shop. *Whatman Grade GF/B Glass Microfiber Filters, Binder Free*. http://www.gelifesciences.com/webapp/wcs/stores/servlet/productById/en/GELifeSciences-de/28418349.

Golden Software, LLC. 2016. *Grapher* (version 7). Golden Software, LLC. www.goldensoftware.com.

Gundelwein, A., T. Müller-Lupp, M. Sommerkorn, E. T. K. Haupt, E.-M. Pfeiffer, and H. Wiechmann. 2007. 'Carbon in Tundra Soils in the Lake Labaz Region of Arctic Siberia'. *European Journal of Soil Science* 58 (5): 1164–74. doi:10.1111/j.1365-2389.2007.00908.x.

Kempf, Bernhard. 2005. 'Dr. Bernhard Kempf - Methodenbeschreibung C, H, N, S'. *Methodenbeschreibung für die C-, H-, N- und S-Bestimmung*. http://www.cup.uni-muenchen.de/oc/kempf/methodenbeschreibung-c-h-n-s.html.

mbm-lehrmittel. 2014. 'QUANTOFIX® Teststäbchen Chlorid'. Web shop. *QUANTOFIX® Teststäbchen Chlorid, Dose à 100 Teststreifen*. http://www.mbm-lehrmittel.de/shopware.php/Basisprodukte/Indikatoren-und-Schnelltests/QUANTOFIX-Teststaebchen-Chlorid-Dose-a-100-Teststreifen.

Pohl, Irmgard, and Josef Zepp. 1966. *Amerika*. Vol. 5. Harms Erdkunde. München / Frankfurt am Main / Berlin / Hamburg / Essen: Paul List.

R Core Team. 2016. *R: A Language and Environment for Statistical Computing* (version R-3.3.1). Vienna, Austria: R Foundation for Statistical Computing. http://www.R-project.org.

Sartorius AG. 2016. 'Sartorius MSU224S-100-DU Analytical Balance - Precision Weighing Balances'. *Sartorius MSU224S-100-DU Analytical*. http://balance.balances.com/scales/746.

———. 2016. 'Sartorius M3P, M3P-000V001 Manual'. Accessed July 21. http://www.sartorius-lab.net/uploads/1/0/6/2/10629561/m3p_manual.pdf.

Strauss, J., L. Schirrmeister, K. Mangelsdorf, L. Eichhorn, S. Wetterich, and U. Herzschuh. 2015. 'Organic-Matter Quality of Deep Permafrost Carbon – a Study from Arctic Siberia'. *Biogeosciences* 12 (7): 2227–45. doi:10.5194/bg-12-2227-2015.

Van Everdingen, R. 2005. 'Multi-Language Glossary of Permafrost and Related Ground-Ice Terms. National Snow and Ice Data Center/World Data Center for Glaciology, Boulder, CO'. *World Wide Web Address: Http://nsidc. Org/fgdc/glossary*, 63–64.

Wagner, Bernd, and Martin Melles. 2001. 'A Holocene Seabird Record from Raffles Sø Sediments, East Greenland, in Response to Climatic and Oceanic Changes'. *Boreas* 30 (3): 228–239.

Wiley Information Services GmbH. 2016. 'Massenspektrometer - Chemgapedia'. http://www.chemgapedia.de/vsengine/glossary/de/massenspektrometer.glos.html.

Zubrzycki, Sebastian. 2012. 'Drilling Frozen Soils in Siberia'. *Polarforschung* 81 (2): 151–153.

## 8. Acknowledgements

# 9. Attachments

## 9.1 Tables

**Table 1**– Analysis results and values of the GL-3-core    ; brown-marked rows indicate unified samples due to small sample mass

| location | sample ID | mean sample depth | dates | brutto wet weight | brutto dry weight | difference wet to dry | ice content (dry-based) | ice content (wet-based) | TN | TC | TOC/TN | TOC | δ13C |
|---|---|---|---|---|---|---|---|---|---|---|---|---|---|
| | | [cm] | | [g] | [g] | [g] | [wt%] | [wt%] | [wt%] | [wt%] | | [wt%] | [‰] |
| Great Lake-3 | GL-3-0-5cm | 2,5 | | 13,8 | 8,4 | 5,4 | 64,3 | 39,1 | 1,8 | 47,9 | 26,6 | 47,4 | -24,93 |
| | GL-3-5-10cm | 7,5 | 652 ± 32 | 18,1 | 6,8 | 11,3 | 166,2 | 62,4 | 1,3 | 46,9 | 37,4 | 46,8 | -22,94 |
| | GL-3-10-15cm | 12,5 | | 19,3 | 7,4 | 11,9 | 160,8 | 61,7 | 1,1 | 47,2 | 41,5 | 47,3 | -22,83 |
| | GL-3-15-20cm | 17,5 | | 28,6 | 8,9 | 19,7 | 221,3 | 68,9 | 0,9 | 46,7 | 52,7 | 46,0 | -22,5 |
| | GL-3-20-24cm | 22 | | 36,5 | 8,5 | 28,0 | 329,4 | 76,7 | 0,8 | 46,4 | 59,0 | 45,7 | -22,26 |
| | GL-3-24-28cm | 26 | | 41,8 | 8,8 | 33,0 | 375,0 | 78,9 | 1,1 | 45,7 | 41,9 | 46,1 | -22,81 |
| | GL-3-28-31cm | 29,5 | | 34,1 | 7,3 | 26,8 | 367,1 | 78,6 | 1,1 | 46,6 | 40,8 | 45,9 | -22,75 |
| | GL-3-31-36cm | 33,5 | | 41,1 | 8,1 | 33,0 | 407,4 | 80,3 | 1,0 | 47,1 | 45,9 | 46,7 | -22,44 |
| | GL-3-36-40cm | 38 | | 41,9 | 8,0 | 33,9 | 423,8 | 80,9 | 0,9 | 46,9 | 49,3 | 46,3 | -22,48 |
| | GL-3-40-48cm | 44 | | 37,3 | 7,7 | 29,6 | 384,4 | 79,4 | 0,8 | 46,3 | 57,3 | 46,3 | -22,06 |
| | GL-3-48-52cm | 50 | 2474 ± 26 | 31,7 | 6,9 | 24,8 | 359,4 | 78,2 | 0,8 | 47,2 | 61,7 | 47,0 | -21,79 |
| | GL-3-52-56cm | 54 | | 33,7 | 7,0 | 26,7 | 381,4 | 79,2 | 0,8 | 47,0 | 56,1 | 46,6 | -22,2 |
| | GL-3-56-60cm | 58 | | 37,6 | 7,4 | 30,2 | 408,1 | 80,3 | 0,9 | 46,9 | 51,4 | 46,7 | -23,25 |
| | GL-3-60-65cm | 62,5 | | 50,9 | 9,1 | 41,8 | 459,3 | 82,1 | 0,9 | 46,3 | 49,3 | 46,2 | -22,76 |
| | GL-3-65-69cm | 67 | | 34,6 | 7,0 | 27,6 | 394,3 | 79,8 | 0,9 | 46,5 | 51,2 | 45,6 | -23,42 |
| | GL-3-69-73cm | 71 | | 30,5 | 7,1 | 23,4 | 329,6 | 76,7 | 1,0 | 47,2 | 46,7 | 47,0 | -24,87 |
| | GL-3-73-77cm | 75 | | 34,1 | 7,6 | 26,5 | 348,7 | 77,7 | 0,9 | 47,6 | 53,6 | 47,6 | -24,83 |
| | GL-3-77-81cm | 79 | | 39,4 | 6,9 | 32,5 | 471,0 | 82,5 | 0,8 | 46,4 | 55,6 | 45,7 | -23,11 |

| | | | | | | | | | | | | |
|---|---|---|---|---|---|---|---|---|---|---|---|---|
| GL-3-81-84cm | 82,5 | | 32,8 | 6,7 | 26,1 | 389,6 | 79,6 | 1,0 | 46,8 | 46,9 | 46,0 | -22,53 |
| GL-3-84-87cm | 85,5 | | 30,2 | 6,4 | 23,8 | 371,9 | 78,8 | 1,1 | 46,9 | 43,3 | 46,3 | -22,47 |
| GL-3-87-91cm | 89 | 2993 ± 33 | 33,4 | 6,3 | 27,1 | 430,2 | 81,1 | 0,9 | 46,6 | 49,6 | 45,8 | -22,48 |
| GL-3-91-95cm | 93 | | 38,0 | 6,9 | 31,1 | 450,7 | 81,8 | 1,1 | 47,6 | 44,0 | 46,9 | -23,82 |
| GL-3-95-99cm | 97 | | 41,3 | 7,5 | 33,8 | 450,7 | 81,8 | 1,0 | 48,3 | 47,4 | 48,2 | -25,32 |
| GL-3-99-102cm | 101,5 | | 25,5 | 6,3 | 19,2 | 304,8 | 75,3 | 1,0 | 47,9 | 48,8 | 47,3 | -25,64 |
| GL-3-102-106cm | 104 | | 36,5 | 7,2 | 29,3 | 406,9 | 80,3 | 1,2 | 47,7 | 39,1 | 46,6 | -24,13 |
| GL-3-106-110cm | 108 | | 40,2 | 8,1 | 32,1 | 396,3 | 79,9 | 1,2 | 48,3 | 41,1 | 48,4 | -23,72 |
| GL-3-110-115cm | 112,5 | | 36,8 | 7,3 | 29,5 | 404,1 | 80,2 | 1,1 | 48,2 | 45,1 | 48,2 | -24,46 |
| GL-3-115-119cm | 117 | | 35,3 | 7,1 | 28,2 | 397,2 | 79,9 | 0,8 | 46,7 | 55,8 | 46,4 | -23,48 |
| GL-3-119-123cm | 121 | | 42,7 | 8,3 | 34,4 | 414,5 | 80,6 | 0,8 | 48,1 | 61,4 | 47,7 | -24,9 |
| GL-3-123-127cm | 125 | | 44,6 | 7,7 | 36,9 | 479,2 | 82,7 | 0,6 | 48,4 | 84,9 | 47,7 | -25,11 |
| GL-3-127-131cm | 129 | 3365 ± 28 | 40,6 | 9,1 | 31,5 | 346,2 | 77,6 | 0,5 | 48,2 | 91,7 | 48,4 | -25,1 |
| GL-3-131-135cm | 133 | | 34,7 | 7,2 | 27,5 | 381,9 | 79,3 | 0,6 | 47,2 | 74,1 | 46,5 | -24,68 |
| GL-3-135-138cm | 136,5 | | 32,0 | 6,7 | 25,3 | 377,6 | 79,1 | 0,7 | 46,7 | 62,1 | 45,4 | -23,99 |
| GL-3-138-141cm | 139,5 | | 30,3 | 6,0 | 24,3 | 405,0 | 80,2 | 0,7 | 45,3 | 62,3 | 44,3 | -22,71 |
| GL-3-141-145cm | 143 | | 29,7 | 6,0 | 23,7 | 395,0 | 79,8 | 0,7 | 45,1 | 61,8 | 43,9 | -23,01 |
| GL-3-145-149cm | 147 | | 34,5 | 5,9 | 28,6 | 484,7 | 82,9 | 0,8 | 45,8 | 57,5 | 44,8 | -23,39 |
| GL-3-149-153cm | 151 | 3417 ± 27 | 34,3 | 6,0 | 28,3 | 471,7 | 82,5 | 0,7 | 45,2 | 63,6 | 44,7 | -23,58 |
| GL-3-153-157cm | 155 | | 35,3 | 6,2 | 29,1 | 469,4 | 82,4 | 0,7 | 45,5 | 58,8 | 44,0 | -22,34 |
| GL-3-157-164cm | 160,3 | | 28,4 | 5,6 | 22,8 | 407,1 | 80,3 | 0,7 | 45,0 | 64,6 | 43,5 | -22,5 |
| GL-3-164-168cm | 166 | | 35,9 | 6,4 | 29,5 | 460,9 | 82,2 | 0,8 | 45,6 | 57,0 | 44,4 | -22,39 |
| GL-3-168-172cm | 170 | | 36,0 | 6,1 | 29,9 | 490,2 | 83,1 | 0,9 | 44,5 | 47,5 | 43,2 | -22,82 |
| GL-3-172-176cm | 174 | | 35,8 | 6,8 | 29,0 | 426,5 | 81,0 | 1,0 | 45,8 | 45,5 | 44,7 | -22,94 |
| GL-3-176-180cm | 178 | | 33,2 | 6,0 | 27,2 | 453,3 | 81,9 | 0,8 | 44,9 | 55,6 | 43,8 | -23,58 |
| GL-3-180-184cm | 182 | | 31,6 | 6,4 | 25,2 | 393,8 | 79,7 | 0,7 | 44,9 | 59,3 | 43,4 | -23,27 |
| GL-3-184-188cm | 186 | | 37,2 | 6,6 | 30,6 | 463,6 | 82,3 | 0,8 | 45,0 | 56,7 | 43,8 | -22,98 |
| GL-3-188-191cm | 189,5 | | 29,3 | 5,6 | 23,7 | 423,2 | 80,9 | 0,8 | 44,6 | 56,7 | 43,5 | -23,29 |
| GL-3-191-198cm | 194,8 | 3553 ± 41 | 29,7 | 5,4 | 24,3 | 450,0 | 81,8 | 0,9 | 43,2 | 48,7 | 42,6 | -23,31 |

| | | | | | | | | | | | | |
|---|---|---|---|---|---|---|---|---|---|---|---|---|
| GL-3-198-201cm | 199,5 | | 20,0 | 5,2 | 14,8 | 284,6 | 74,0 | 0,8 | 44,7 | 54,3 | 43,1 | -23,63 |
| GL-3-201-205cm | 203 | | 33,9 | 5,9 | 28,0 | 474,6 | 82,6 | 0,8 | 44,2 | 56,6 | 44,3 | -23,63 |
| GL-3-205-212cm | 208,3 | | 27,8 | 5,6 | 22,2 | 396,4 | 79,9 | 1,0 | 44,4 | 46,1 | 44,7 | -23,09 |
| GL-3-212-217cm | 214,5 | | 45,3 | 7,5 | 37,8 | 504,0 | 83,4 | 1,0 | 44,1 | 45,4 | 44,0 | -23,37 |
| GL-3-217-221cm | 219 | | 30,9 | 5,9 | 25,0 | 423,7 | 80,9 | 1,0 | 43,8 | 44,2 | 43,9 | -22,96 |
| GL-3-221-224cm | 222,5 | | 29,0 | 6,0 | 23,0 | 383,3 | 79,3 | 1,5 | 46,1 | 32,4 | 47,1 | -26,17 |
| GL-3-224-227cm | 225,5 | | 24,0 | 5,7 | 18,3 | 321,1 | 76,3 | 1,9 | 46,8 | 24,7 | 47,9 | -26,59 |
| GL-3-227-231cm | 229 | 3605 ± 26 | 32,0 | 6,4 | 25,6 | 400,0 | 80,0 | 1,5 | 45,5 | 30,8 | 45,5 | -25,16 |
| GL-3-231-235cm | 233 | | 36,9 | 6,4 | 30,5 | 476,6 | 82,7 | 0,8 | 42,9 | 52,1 | 42,9 | -22,4 |
| GL-3-235-242cm | 238,3 | | 23,5 | 5,3 | 18,2 | 343,4 | 77,4 | 1,1 | 43,1 | 37,4 | 42,8 | -22,48 |
| GL-3-242-248cm | 245 | | 19,1 | 5,0 | 14,1 | 282,0 | 73,8 | 1,1 | 42,9 | 39,5 | 43,6 | -22,56 |
| GL-3-248-252cm | 250 | 3720 ± 31 | 32,3 | 6,2 | 26,1 | 421,0 | 80,8 | 1,3 | 43,1 | 33,7 | 43,1 | -22,35 |
| GL-3-252-255cm | 253,5 | | 27,8 | 5,4 | 22,4 | 414,8 | 80,6 | 1,2 | 43,0 | 36,1 | 42,4 | -23,62 |
| GL-3-255-260cm | 257,5 | | 41,6 | 6,6 | 35,0 | 530,3 | 84,1 | 1,1 | 42,8 | 38,4 | 42,2 | -23,25 |
| GL-3-260-265cm | 262,5 | | 41,8 | 6,2 | 35,6 | 574,2 | 85,2 | 1,0 | 43,4 | 42,1 | 42,9 | -23,3 |
| GL-3-265-267cm | 266 | | 11,1 | 4,8 | 6,3 | 131,3 | 56,8 | 1,2 | 42,7 | 36,5 | 42,7 | -22,73 |
| GL-3-267-271cm | 269 | 3568 ± 39 | 36,4 | 6,2 | 30,2 | 487,1 | 83,0 | 1,2 | 43,1 | 37,2 | 42,9 | -22,66 |
| GL-3-271-275cm | 273 | | 36,6 | 6,3 | 30,3 | 481,0 | 82,8 | 1,2 | 42,9 | 33,8 | 42,1 | -22,4 |
| GL-3-275-280cm | 277,5 | | 39,2 | 6,8 | 32,4 | 476,5 | 82,7 | 1,3 | 43,4 | 31,7 | 42,6 | -21,71 |
| GL-3-280-285cm | 282,5 | | 42,2 | 6,9 | 35,3 | 511,6 | 83,6 | 1,1 | 43,6 | 38,7 | 43,4 | -22,45 |
| GL-3-285-290cm | 287,5 | | 38,7 | 6,9 | 31,8 | 460,9 | 82,2 | 1,4 | 43,8 | 30,9 | 43,7 | -20,98 |
| GL-3-290-295cm | 292,5 | | 46,1 | 7,0 | 39,1 | 558,6 | 84,8 | 1,3 | 43,4 | 33,3 | 43,3 | -20,84 |
| GL-3-295-300cm | 297,5 | | 42,0 | 6,8 | 35,2 | 517,6 | 83,8 | 1,3 | 43,5 | 34,7 | 43,7 | -20,8 |
| GL-3-300-305cm | 302,5 | 3802 ± 41 | 47,0 | 6,3 | 40,7 | 646,0 | 86,6 | 1,2 | 44,2 | 37,5 | 43,8 | -20,73 |
| GL-3-305-309cm | 307 | | 34,3 | 5,8 | 28,5 | 491,4 | 83,1 | 1,3 | 43,4 | 33,7 | 43,2 | -20,93 |
| GL-3-309-313cm | 311 | | 30,6 | 5,7 | 24,9 | 436,8 | 81,4 | 1,2 | 43,6 | 36,8 | 42,9 | -21,05 |
| GL-3-313-316cm | 314,5 | | 26,1 | 5,3 | 20,8 | 392,5 | 79,7 | 1,5 | 44,1 | 30,4 | 44,6 | -21,56 |
| GL-3-316-320cm | 318 | 3855 ± 30 | 36,9 | 6,2 | 30,7 | 495,2 | 83,2 | 1,6 | 43,8 | 28,1 | 44,1 | -23,65 |

## 9.2 German summary / deutsche Zusammenfassung

Diese Arbeit befasst sich mit dem Abbau organischer Substanz und damit einhergehender Bodenbildung im von Eiskeil-Polygonen geprägten Permafrost im Gebiet von Thule in Nordwest-Grönland. Dazu wurde ein Permafrost-Bohrkern aus besagtem Gebiet untersucht, der dort im August 2015 im Rahmen des dänischen NOW Projektes gewonnen wurde.

Die Bildung dieser Eiskeil-Polygone, die Akkumulation von Bodenmaterial sowie die Verbindung zu ortsansässigen Vogelkolonien sind Gegenstand der Untersuchungen im Rahmen dieser Arbeit.

Es wurde festgestellt, dass der Permafrost in diesem Untersuchungsgebiet ungewöhnlich hohe Stickstoffkonzentrationen aufweist. Außerdem ist dieser Permafrost sehr eishaltig.

Die aus diesem Bohrkern gewonnenen Proben wurden im Labor hinsichtlich des Eisgehaltes, des Kernalters, des Kohlenstoff- sowie Stickstoffgehaltes, des Gehaltes an organischem Kohlenstoff sowie des Isotopenverhältnisses in organischem Kohlenstoff (TOC) und Stickstoff (TN) untersucht.

Dabei ergab sich ein Bild von überwiegend konstantem Zustand aller Parameter mit einigen Abweichungen in je nach Parameter variierender Tiefe.

Außerdem wurde festgestellt, dass vor ca. 3000 Jahren eine massive Veränderung in diesem Permafrost-System stattgefunden haben muss, da sich zu diesem Zeitpunkt die Akkumulationsrate des Bodens maßgeblich änderte. Was genau jedoch diese Veränderung herbeigeführt hat und damit die Bodenbildung so drastisch beeinflusste muss noch weitergehend untersucht werden

Des Weiteren wurden Hinweise auf den großen Einfluss der ansässigen Seevogelkolonien auf die lokalen Bodenparameter gefunden. Insbesondere die hohen Stickstoffgehalte lassen vermuten, dass die Exkremente jener Vogelkolonien die ursprüngliche Quelle organischen Materials sind, welches dann zersetzt wurde und schlussendlich den Permafrost in diesem Untersuchungsgebiet gebildet hat.

Zusätzlich wurde eine zeitlich begrenzte Veränderung des Isotopenverhältnisses im Kohlenstoff entdeckt, was eventuell auf eine externe Kohlenstoffquelle hindeutet und somit möglicherweise Hinweise auf die Entwicklung des gesamten regionalen Vogelbestandes geben kann.

## 9.3 Independence statement / Eigenständigkeitserklärung

Eidesstattliche Erklärung zur Bachelorarbeit

Ich versichere, diese Arbeit selbständig und lediglich unter Benutzung der angegebenen Quellen und Hilfsmittel verfasst zu haben.

Alle Stellen, die wörtlich oder sinngemäß aus veröffentlichten oder noch nicht veröffentlichten Quellen entnommen sind, sind als solche kenntlich gemacht.

Die Zeichnungen oder Abbildungen in dieser Arbeit sind von mir selbst erstellt worden oder mit einem entsprechenden Quellennachweis versehen.

Ich erkläre weiterhin, dass die vorliegende Arbeit noch nicht im Rahmen eines anderen Prüfungsverfahrens eingereicht wurde.

Potsdam, den _____                    _____

Statutory Declaration

I declare that I have authored this thesis independently, that I have not used other than the declared sources / resources

and that I have explicitly marked all material which has been quoted either literally or by content from the used sources.

Furthermore I declare that this thesis has not been submitted for any other exam.

Potsdam, _____                    _____